Address correspondence to Dr Robert S. Miletich, University at Buffalo, 105 Parker Hall, 3435 Main St, Buffalo, NY 14214, *miletich@buffalo.edu*.

Relationship Disclosure: Dr Miletich serves on the editorial board of the *Journal of Neuroimaging* and receives research/grant support from the William E. Mabie, DDS, and Grace S. Mabie Fund.

Unlabeled Use of Products/Investigational Use Disclosure: Dr Miletich reports no disclosure.

Positron Emission Tomography and Single-Photon Emission Computed Tomography in Neurology

Robert S. Miletich, MD, PhD, FAAAS

ABSTRACT

Purpose of Review: Positron emission tomography (PET) and single-photon emission computed tomography (SPECT) are now available for routine clinical applications in neurology. This article discusses their diagnostic use in dementia, brain tumors, epilepsy, parkinsonism, cerebrovascular disease, and traumatic brain injury.

Recent Findings: Neuromolecular imaging, also known as nuclear neurology, involves clinical imaging of both basal regional physiology (perfusion, metabolism, and transport mechanisms) and specific neurochemical physiology (currently, only the dopamine transporter). This article serves as an introduction to neuromolecular imaging, reviewing the literature supplemented by the author's experience.

Summary: Neurologic PET and SPECT are no longer restricted to the research realm. These modalities have high diagnostic accuracy.

Continuum (Minneap Minn) 2016;22(5):1636–1654.

INTRODUCTION

This article discusses the clinical application of neuromolecular imaging, also known as nuclear neurology, focusing on tomographic methods that are currently available and accessible in routine clinical care, if regional expertise exists. Planar scintigraphy methods, in which a two-dimensional image is created of a three-dimensional object, such as in nuclear cisternography or spine bone scans, are not reviewed in this article. The focus is on literature from the past 5 years supplemented by the author's clinical experience. Clinical neuromolecular imaging examines the central nervous system distribution of US Food and Drug Administration (FDA)–approved radiopharmaceuticals for positron emission tomography (PET) and single-photon emission computed tomography (SPECT). In the author's experience, medical insurance usually reimburses for both the radiopharmaceuticals and the imaging tests reviewed in this article.

SPECT utilizes standard nuclear medicine cameras for which tomographic methods are enabled. SPECT capability is ubiquitous, as all nuclear medicine departments in nearly every hospital in the United States have such cameras. The most common radioisotopes used in SPECT are technetium 99m (^{99m}Tc), iodine 123 (^{123}I), thallium 201 (^{201}Tl), and indium 111 (^{111}In). These radioisotopes are incorporated

into molecules that trace a physiologic process. Physiologic processes that can be measured in the clinical arena with SPECT include cerebral perfusion with exametazime Tc 99m or bicisate Tc 99m, dopamine transporter (DAT) concentrations with ioflupane I 123, brain tumor uptake with thallous chloride Tl 201, and CSF hydrodynamics with diethylenetriamine pentaacetic acid (DTPA) In 111.

PET requires specialized cameras, as the physical process requires coincident detection of two high-energy 511-keV photons. The only widely available radioisotope for clinical PET is fluorine 18 (^{18}F), which, because of its long half-life of 110 minutes, can be disseminated from regional distribution centers. Other radioisotopes that may be used clinically have much shorter half-lives, requiring on-site or local production; these are not reviewed in this article. The only physiologic process that can be assessed clinically by PET is cerebral glucose metabolism with fludeoxyglucose F 18 (FDG).

Neuromolecular imaging can measure some aspect of a pathologic process within the brain, but it can also measure the physiologic effects of that pathology on the functioning of cerebral parenchyma. Both types of measurements provide useful diagnostic information. Because of the nearly stoichiometric relationship between regional neuronal synaptic activity, regional perfusion, and regional glucose metabolism, measuring the latter two provides information about regional brain activity. Currently neuromolecular imaging can assay a number of physiologic processes clinically. These assays can serve as biomarkers for the disease process. However, the diagnostic accuracy for any imaging biomarker is as dependent on how the biomarker is measured as it is on the biomarker itself.[1] Neuromolecular imaging is specialized testing requiring specific expertise. As much can be gained diagnostically from the visual interpretation of these images by competent interpreters as from statistically rigorous methodology. Visual interpretation is the typical experience in the clinical realm.

To review all potential applications of neuromolecular imaging would require review of all neurologic disorders; this article reviews the most common indications for which clinical reimbursement exists: dementia, brain tumors, epilepsy, parkinsonism, cerebrovascular disease, and traumatic brain injury (TBI). **Table 12-1** lists indications and the type of neuromolecular imaging used in these disorders.

KEY POINT

- Neuromolecular imaging can measure some aspect of a pathologic process within the brain, but it can also measure the physiologic effects of that pathology on the functioning of cerebral parenchyma. Both types of measurements provide useful diagnostic information.

DEMENTIA

With the aging populations of industrial and postindustrial societies throughout the world, age-related disorders, including neurodegenerative disorders and specifically Alzheimer disease (AD), are becoming public health epidemics. Effective therapies for neurodegenerative disorders have not been developed because the basic pathophysiology of the disorders is not understood. Clinical trials of new therapies are confounded by the presence of multiple diseases that show phenotypically similar clinical presentations. Currently, the field is searching for biomarkers that can properly diagnose these diseases, particularly in the early stages when abortive therapy will be most effective. Neuromolecular imaging provides the potential for sensitive imaging biomarkers in dementia. Two indications for neuromolecular imaging exist in dementia: early diagnosis and differential diagnosis.

With the realization that neurodegenerative dementia has a prodromal

KEY POINT

- Positive positron emission tomography amyloid imaging is a biomarker of brain amyloid-β deposition, and fludeoxyglucose positron emission tomography hypometabolism in the temporal and parietal cortices and MRI atrophy in the temporal and parietal lobes are biomarkers of neuronal degeneration or injury.

TABLE 12-1 Indications for Clinically Available Neuromolecular Imaging Tests

Disorder	Indications	PET	SPECT
Dementia	Early diagnosis, differential diagnosis	FDG	Bicisate, exametazime
Brain tumors	Grading, staging, tumor localization, mass lesion diagnosis, tumor recurrence versus treatment effect, therapy efficacy evaluation, malignant degeneration diagnosis, prognostication	FDG	Thallium
Epilepsy	Episodic neurologic syndrome diagnosis, localization of seizure focus	FDG	Bicisate, exametazime
Parkinsonism	Early diagnosis, differential diagnosis	FDG	Ioflupane, bicisate, exametazime
Cerebrovascular disease	Cellular viability, cellular ischemia		Bicisate
Traumatic brain injury	Injury identification	FDG	Bicisate

FDG = fludeoxyglucose; PET = positron emission tomography; SPECT = single-photon emission computed tomography.

phase, a new diagnostic category called mild cognitive impairment (MCI) gained wide acceptance. In the past 30 years, the importance of neuroimaging in the diagnosis of dementia has also been accepted.[2] As such, a joint task force was convened by the National Institute on Aging (NIA) and the Alzheimer's Association (AA) to revise the classic 1984 National Institute of Neurological and Communicative Disorders (NINCDS)–Alzheimer's Disease and Related Disorders Association (ADRDA) criteria for the diagnosis of AD in both dementia and MCI.[3,4] These criteria now include core clinical features and biomarkers of the pathophysiologic process. The latter includes two classes of evidence: biomarkers of brain amyloid-β deposition and biomarkers of neuronal degeneration or injury. In imaging, positive PET amyloid imaging is a biomarker of brain amyloid-β deposition, and FDG-PET hypometabolism in the temporal and parietal cortices and MRI atrophy in the temporal and parietal lobes are biomarkers of neuronal degeneration or injury.

Reviews have summarized diagnostic accuracy for both perfusion SPECT and FDG-PET in the diagnosis of AD. Perfusion SPECT has been reported to have sensitivities of 65% to 85% and specificities of 72% to 87%. FDG-PET sensitivities of 75% to 99% and specificities of 71% to 93% have been reported. In general, PET has higher diagnostic accuracy (an average of 10% higher) than SPECT.[5] Another review essentially replicated these findings, with FDG-PET in AD versus controls showing 89% to 99% sensitivities and 60% to 87% sensitivities.[6]

Cerebral perfusion SPECT has variable efficacy in distinguishing AD from other diseases, usually less effective than in comparisons of AD with healthy controls. For distinguishing AD from healthy controls, exametazime SPECT had 76% sensitivity and 85% specificity. These values were 80% and 80% for frontotemporal dementia, 75% and 72% for vascular dementia, and 70% and 76% for dementia with Lewy bodies (DLB).[7] SPECT had 79% accuracy for distinguishing AD from other dementing illnesses.[6] Overall, the few recent publications on MCI have shown intermediate changes between dementias and healthy controls.[8] Nonetheless, because neuromolecular imaging captures the functional status of the brain, it has the capability for early diagnosis (**Case 12-1**) and differential diagnosis (**Figure 12-2**) in MCI.

Three amyloid imaging markers, florbetapir, flutemetamol, and florbetaben, have been approved by the FDA, all tagged by ^{18}F. Amyloid imaging has shown high correlation between regional amyloid tracer uptake and postmortem insoluble amyloid deposits. Patients with AD have 50% to 90% higher gray matter concentrations of amyloid tracers than controls. Amyloid imaging may be useful in the differential diagnosis of dementia as amyloid accumulations in frontotemporal lobar degeneration are low, similar to healthy controls.[8] However, amyloid imaging's specificity is not fully defined at this time and more research is needed. For instance, approximately 25% of patients with Parkinson disease (PD) with dementia and DLB had positive amyloid scans, similar to AD.[12] Although the FDA has approved amyloid imaging agents, Medicare has not approved these studies for reimbursement outside of the research setting. Although 80% to 100% sensitivity and specificity have been reported using the amyloid imaging research radiopharmaceutical carbon 11–labeled Pittsburgh Compound B (^{11}C-PiB), this diagnostic accuracy is dependent on age as an age-related increased prevalence of amyloid tracer uptake exists, with up to 40% of asymptomatic people over 70 years of age having high cortical PiB uptake.[6,13] Amyloid imaging also shows little significant change over time and is poorly correlated with clinical progression of disease, in contrast to atrophy on MRI and cerebral perfusion and metabolism worsening with disease progression. A potential application of amyloid imaging is prognosticating AD development in patients with MCI or even in asymptomatic individuals, but this has not been established.[13] Given the uncertainties of the pathophysiologic process of AD, it remains unclear what the diagnostic certainty for amyloid imaging will be. Although it is likely that amyloid imaging will have very good negative predictive value, a likely poor positive predictive value may hinder its usefulness.

It has been proposed that examination of the dopamine system with DAT agents can help in the differential diagnosis of AD from DLB or PD dementia,[12] but few studies have been published at this time.

A comprehensive meta-analysis review of literature from January 1990 to March 2010 that examined diagnostic biomarkers for AD, including CSF, clinical features, MRI, SPECT, and FDG-PET, showed that as compared to controls without dementia, FDG-PET had the highest area under the receiver operating characteristic curve (AUROC) at 0.96, with 90% sensitivity and 89% specificity. FDG-PET was also best in discriminating AD from other dementias, with 0.91 AUROC, 92% sensitivity, and 78% specificity. The performance of SPECT, MRI, and CSF phosphorylated tau concentrations

KEY POINT

- Patterns of central nervous system dysfunction shown on neuromolecular imaging usually develop early in the disease course of dementia, facilitating early diagnosis.

Case 12-1

A 67-year-old man developed confusion postoperatively following endovascular repair of an abdominal aortic aneurysm. The confusion cleared, but he and his wife noted short-term memory problems that progressively worsened over the subsequent year. He also developed difficulties with calculations and multitasking. His wife noted that he no longer did well under pressure situations. He was a retired attorney and remained independent in activities of daily living. Past medical history was significant for hypercholesterolemia, hypertension, and vitamin B_{12} and vitamin D deficiencies. All four disorders had been medically corrected or controlled by the time of the fludeoxyglucose positron emission tomography (FDG-PET) scan; MRI showed moderate diffuse atrophy. He had recently scored 25 out of 30 on the Mini-Mental State Examination (MMSE) and had been diagnosed with amnestic mild cognitive impairment. FDG-PET/CT revealed mild diffuse atrophy on CT and a selective pattern of association cortex hypometabolism, worst posteriorly. Severe decreases were shown in the lateral parietal cortex (**Figure 12-1A**) and medial parietal cortex (**Figure 12-1B**). Severe hypometabolism in the inferior temporal cortex, moderate hypometabolism in lateral temporal cortex, and mild decreases in frontal cortex were also present.

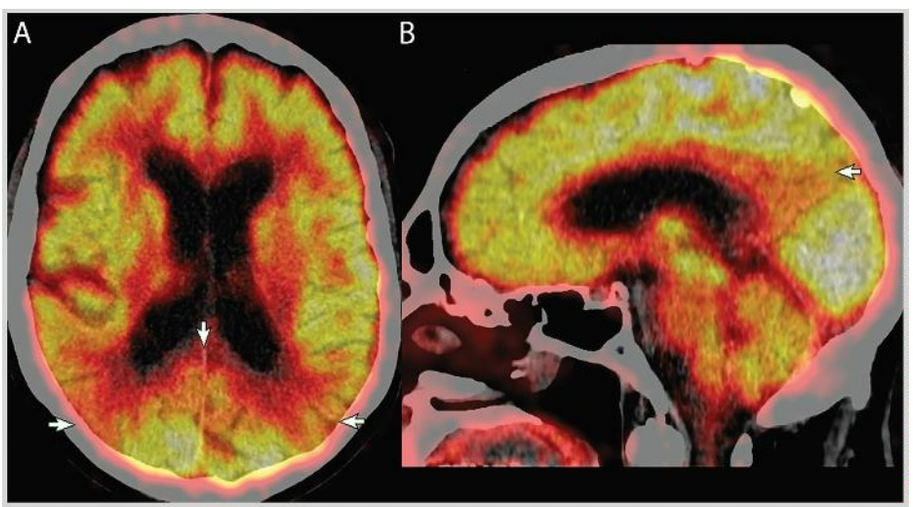

FIGURE 12-1 Imaging of the patient in **Case 12-1.** Fludeoxyglucose positron emission tomography (FDG-PET)/CT with fused CT in gray scale and PET in color scale in the transverse (*A*) and sagittal (*B*) planes. Severe hypometabolism can be seen in the medial parietal cortex (*A, down-pointing arrow*; *B, arrow*), and lateral parietal cortex (*A, horizontal arrows*). Bright intensity or hot coloration (*white, yellow*) in PET indicates high tracer localization and thus higher amounts of glucose metabolism. Low intensity or cold coloration (*black, orange*) indicates low amounts.

Comment. This case demonstrates the use of FDG-PET/CT in supporting the diagnosis of prodromal Alzheimer disease in mild cognitive impairment. Recent literature analyzing diagnostic testing, disease risk factors, and postmortem pathology have revealed that besides Alzheimer disease, mild cognitive impairment can result from multiple other disorders, individually or as comorbidities.[9–11] FDG-PET/CT revealed association cortex dysfunction in a pattern unique to Alzheimer disease. This pattern had no CT correlate in that the atrophy seen was diffuse.

were similar to one another, with AUROC of 0.85 to 0.86.[14]

AD is a global brain disorder. The often-stated criteria for making the neuromolecular imaging diagnosis of AD has been hypometabolism or hypoperfusion in the temporal and parietal cortices. Although this certainly is

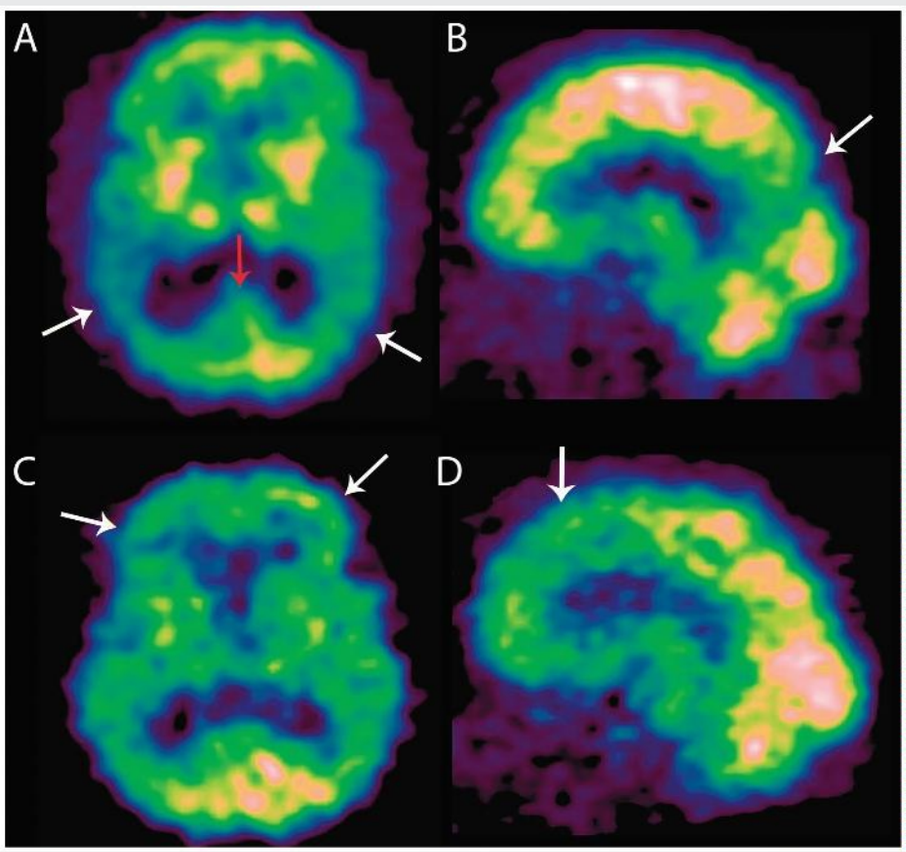

FIGURE 12-2 Two examples of the neurodegenerative patterns of Alzheimer disease (*A, B*) and frontotemporal lobar degeneration (*C, D*) in cerebral perfusion bicisate single-photon emission computed tomography (SPECT) from transverse (*A, C*) and sagittal planes (*B, D*). Regions of maximal involvement in the medial parietal cortex (*A, red arrow*; *B, arrow*), lateral temporal and parietal cortices (*A, white arrows*), medial frontal cortex (*D, arrow*), and polar and lateral frontal cortex (*C, arrows*) can be seen. Images are of a 70-year-old woman (*A, B*) and an 85-year-old man (*C, D*) both with a 1-year history of short-term memory impairment. Both had been diagnosed with mild cognitive impairment and maintained intact affairs of daily living. Bright intensity or hot coloration (*white, yellow*) in SPECT indicates high tracer localization and thus higher amounts of cerebral perfusion. Low intensity or cold coloration (*black, purple, blue-green*) indicates low amounts.

needed, it is an inadequate characterization of the array of changes that are seen functionally on neuromolecular imaging in AD. These findings include a widespread, but posteriorly dominant, asymmetric association cortex hypofunction with relative preservation of function in the primary cortices. Many disorders cause decreased function of the association cortex, which is called the global brain impairment pattern. Many global brain impairment subpatterns exist, which help distinguish between the different disorders. In the previously mentioned literature, neuromolecular imaging specificities are often lower than the sensitivities. This is because other disorders have a predilection for affecting the temporal and parietal cortices. In the author's clinical practice, the biggest confounder is small vessel disease.[15]

BRAIN TUMORS

Approximately 50,000 people are diagnosed with primary brain tumors in the United States annually and 140,000 with metastatic brain tumors.

KEY POINTS

- Each dementing illness has its own pattern of central nervous system dysfunction on neuromolecular imaging, facilitating differential diagnosis.
- The typical imaging pattern for Alzheimer disease is a posteriorly dominant asymmetric association cortex hypofunction, worst in temporal and parietal cortices, with important involvement of the medial parietal cortex. Function is better preserved in primary cortex and subcortical gray matter structures.

KEY POINTS

- The biological behavior of tumors is reflected in their glucose metabolic profile.
- The interpretation of fludeoxyglucose positron emission tomography requires multimodal cross-correlation.

Gliomas were the first human neoplasm for which the diagnostic utility of FDG-PET was shown by the Giovanni Di Chiro group in 1982.[15] The foundation for this was laid by Otto Warburg in the 1930s, who showed increasing glucose utilization and glycolysis in many different body cancers with increasing malignancy and anaplasia. This is now coined the *Warburg theory*, and it remains the basis for the use of FDG-PET in oncology. Having a noninvasive measure of the biological behavior of tumors is critical for rational management of these disorders.

The indications for FDG-PET in brain tumors include tumor grading, tumor staging, tumor localization, the differential diagnosis of cerebral mass lesions, distinguishing between tumor recurrence versus treatment effect, therapy efficacy evaluation, early diagnosis of malignant degeneration, and prognostication.[15,16] The author's experience is that FDG-PET is a useful technique for all of these indications. Therapy must be titrated for the tumor grade. Targeted therapies require knowledge of tumor location and spread. MRI is very sensitive to structural changes but often is not specific and may not distinguish where neoplasm actually resides within a lesion bed. It often cannot distinguish tissue inflammation or necrosis from neoplasm, a distinction needed for therapy evaluation or planning. Low-grade gliomas quite often undergo malignant degeneration to a higher-grade tumor. Timely diagnosis of such transformation can improve outcomes. Finally, because FDG-PET is an assay of high fidelity for the tumor's biological behavior, a more accurate prognosis is thus provided.

It is true that FDG-PET is not easy to interpret given that the milieu is the cerebrum, the most metabolically active organ in the body. It is easy to misinterpret these studies in the absence of sufficient training and experience. In the management of patients with brain tumors, MRI remains the standard imaging modality, in particular using contrast-enhanced sequences. These have high sensitivity but often low specificity. This often leads to the diagnostic conundrum of assessing the presence of treatment effect versus tumor recurrence in patients with known brain tumors. This is the most common indication for FDG-PET in the author's experience. As such, the interpretation of FDG-PET requires multimodal cross-correlation. More diagnostic information is extracted from PET by correlating it to MRI. FDG-PET is complementary to MRI in that it adds value in defining the biological behavior of the lesion field.

Much of the formative work on the efficacy of FDG-PET in brain tumors was published decades ago by the Di Chiro National Institutes of Health group. More recent work has replicated this earlier work and has shown the high diagnostic accuracy of FDG-PET for grading tumors, assessing tumor progression, and distinguishing tumor recurrence versus treatment effect in previously treated patients with brain tumors.[17] For example, using tumor FDG uptake that is greater than or equal to 0.6 times the values in gray matter or 1.5 times the values in white matter resulted in 94% sensitivity and 77% specificity for distinguishing high-grade from low-grade neoplasms.[16] For the diagnosis of tumor recurrence versus treatment effect, sensitivities of 80% to 86% and specificities of 40% to 88% have been reported in the literature (**Case 12-2**).[16] This wide range of reported values may be because of variability of interpretative skills, as discussed previously. By characterizing the biological behavior of brain

Case 12-2

A 57-year-old woman who underwent resection of a left occipital lobe glioblastoma multiforme 2 years previously, followed by concurrent chemoradiation and 24 cycles of adjuvant temozolomide, was found to have a new contrast-enhancing lesion on MRI 2 months after completion of her last cycle of temozolomide. Fludeoxyglucose positron emission tomography (FDG-PET)/CT was requested for evaluation of tumor recurrence versus treatment effect. PET (**Figures 12-3A** and **12-3C**) clearly revealed a 7-mm hypermetabolic focus at the MRI contrast-enhancing site (**Figure 12-3D**). CT showed a faint cortical hypoattenuation (**Figure 12-3B**). The surrounding cortex was hypometabolic. These findings were consistent with tumor recurrence in the right medial parietal cortex, contralateral to the original neoplasm. Stereotactic radiosurgery was planned.

Comment. This case illustrates a number of points. Small lesions can be assessed with modern PET/CT cameras because of improved spatial resolution. PET is rarely read in isolation of any other modalities. To extract the maximum amount of diagnostic information from functional imaging, cross-correlation to structural imaging is needed. The interpretation of brain tumor studies is based both on tumor bed changes and the effects on the cerebral parenchyma.

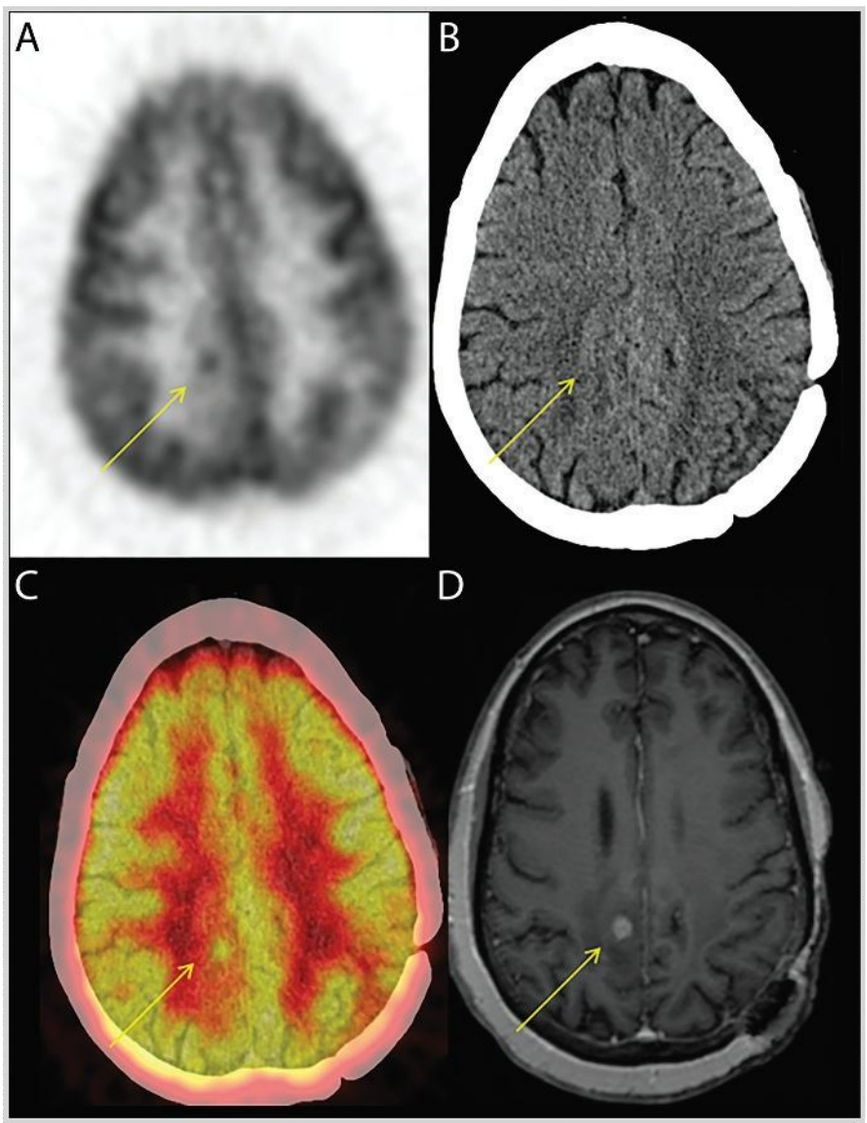

FIGURE 12-3 Multimodal imaging of the patient in **Case 12-2** with fludeoxyglucose positron emission tomography (FDG-PET) (*A*), CT (*B*), fused PET and CT (*C*), and gadolinium-enhanced T1-weighted MRI (*D*). A 7-mm focus of hypermetabolism is seen (*A, C, arrows*) at the site of MRI enhancement (*D, arrow*). Mild hypoattenuation can be seen at this site on CT (*B, arrow*). This focus is surrounded by hypometabolic cortical ribbons. The findings are consistent with recurrence of high-grade glioma and diaschisis of neighboring gray matter. In *panel A*, darker intensity indicates higher amounts of glucose metabolism. In *panel C*, bright intensity or hot coloration (*white, yellow*) indicates higher amounts of glucose metabolism.

KEY POINT

- Neuromolecular imaging has proven usefulness in the noninvasive identification of the epileptic zone in candidates for resective epileptic surgery.

tumors, FDG-PET provides prognostic information. For example, high FDG uptake in glioblastomas was associated with a 29% 1-year survival, while low FDG uptake was associated with a 94% 1-year survival.[18] This essentially replicates the findings reported by the Di Chiro group 30 years ago.

Another camp of opinion exists in the literature that denigrates the effectiveness of FDG-PET in providing useful clinical management information in brain tumors. This group has discouraged use of FDG-PET for assessment of glioblastoma progression[19] or for assessing tumor progression versus treatment effect following radiosurgery.[20] These negative pronouncements may be related to the interpretative difficulties posed by evaluating glucose metabolism within the brain. FDG-PET diagnosis is not made simply by the presence or absence of tumoral FDG. It is a multimodal cross-correlative evaluation that assesses magnitude, pattern, morphology, location, and even temporal behavior of this uptake relative to the structural changes shown on MRI. Also critical in this evaluation are the effects on the surrounding parenchyma. High diagnostic accuracy exists with the proper interpretative scheme.

Because of reported difficulties with FDG, a movement for imaging brain tumors with radioactive amino acids has developed, primarily in Europe. Given the greater contrast of uptake between neoplasm and brain parenchyma, imaging with radioactive amino acids is easier to read. However, the grading capability of these images has been questioned in the literature.[21] In the opinion of this author, with an experienced neuromolecular imager, FDG provides high diagnostic accuracy. No other PET and SPECT tracers have been definitively shown to be diagnostically advantageous as compared to FDG,[18] and no PET agents are FDA approved for amino acid imaging.

SPECT with [^{201}Tl]thallous chloride is also a useful neuromolecular imaging technique for brain tumors. Although the sensitivities and specificities are not as high as those of FDG-PET, they have been reported in the 80% range, indicating a useful diagnostic test. SPECT with [^{201}Tl]thallous chloride has been recommended for assessment of glioblastoma progression.[19] Thallium is treated as a potassium analogue by the blood-brain barrier and, as such, gains entry into the brain only with blood-brain barrier disruption. This simplifies interpretation, as it becomes a matter of hot spot identification.

EPILEPSY

Epilepsy affects 1% to 2% of the population. At least 30% of patients with epilepsy will fail to adequately respond to antiepileptic drugs. Surgical treatment remains an option in these patients. Two main indications exist for neuromolecular imaging in epilepsy. One is to assist in the differential diagnosis of episodic syndromes that may or may not be due to epilepsy. The second is to help localize the epileptogenic zone in candidates for surgical resection of a seizure focus. The first indication has become an integral part of the author's clinical practice; unfortunately, no well-characterized published data exist on this use of neuromolecular imaging. However, the presurgical evaluation indication is well established.[22–24]

Neuromolecular imaging has proven usefulness in the noninvasive identification of the epileptic zone in candidates for resective epileptic surgery. This localization requires a multimodal investigation that includes electrophysiology, structural imaging, and functional imaging and may include

invasive neurosurgical diagnostic techniques. Interictal FDG-PET and both ictal and interictal SPECT are now routinely performed in surgical epilepsy centers throughout the world. Neuromolecular imaging has high sensitivity, with ictal SPECT at 96%, interictal SPECT at 44%, postictal SPECT at 75%, and interictal FDG-PET on modern equipment up to 90% for temporal lobe epilepsy and 67% for extratemporal epilepsy (**Case 12-3**).[16]

The combination of interictal and ictal SPECT, with or without MRI, using standard computer imaging technology increases the diagnostic accuracy of epileptic zone localization. This image processing is done at surgical epilepsy centers throughout the world. Many different systems have been developed. Subtraction ictal SPECT coregistered to MRI (SISCOM), developed at the Mayo Clinic, is the most widely known, but other methodologies exist.[25] During ictus, seizure foci demonstrate hyperperfusion. The purpose of combining the ictal and interictal SPECT images is to identify this site of ictal-activated hyperperfusion. This is done by subtracting the interictal image volume from the ictal image volume. The difference is ictal activation. All of these techniques require three-dimensional registration of image sets, followed by proportional normalization, which then allows algebraic manipulation of the interictal and ictal images. The final product is parametric images of ictal activation (**Figures 12-4C** and **12-4D**). Even ictal deactivation parametric images can be created. Examining both ictal activation and ictal deactivation parametric images can provide diagnostic information. The greatest challenge in performing ictal SPECT is in injecting radiotracer as close to the time of seizure onset as possible. Four different patterns of ictal activation and deactivation can be seen based on the timing of the bicisate injection relative to seizure onset: focal ictal activation, lobar or even more widespread ictal activation, widespread ictal deactivation, and focal ictal deactivation. The first has the greatest fidelity for epileptic zone characterization, but diagnostic information is present in each pattern.

For many patients, noninvasive techniques may be sufficient to guide surgery for the site of surgical resection. However, if localization is not possible, neuromolecular imaging may be able to regionalize or lateralize the epileptogenic zone, which can minimize the extent of subsequent invasive diagnostic techniques. Neuromolecular imaging is particularly useful when MRI is either normal or shows multiple lesions, any one of which could be the epileptic zone.

Neuromolecular imaging is also useful in epileptic syndromes, such as in epileptic spasms with the EEG pattern of hypsarrhythmia. The underlying pathology is variable and can be due to either multifocal or unifocal cortical lesions, resection of which may cure or control epilepsy.[24] Other syndromes with similar considerations are tuberous sclerosis, Sturge-Weber syndrome, various congenital malformations, and even Rasmussen encephalitis. The goal in all of these is to identify a resectable epileptic zone.

PARKINSONISM

The clinical diagnosis of PD is incorrect 20% of the time.[26] Misdiagnosis is even greater for the atypical parkinsonian syndromes. This differential diagnosis problem arises because of the large number of disorders causing parkinsonism.[27] These include the Lewy body diseases of PD and DLB; the atypical parkinsonian syndromes multiple system atrophy (MSA), progressive supranuclear palsy (PSP),

KEY POINTS

- Ictal single-photon emission computed tomography and interictal positron emission tomography can help localize seizure foci in the presurgical evaluation of candidates for epilepsy surgery.
- A computer-generated combination of ictal single-photon emission computed tomography (SPECT), interictal SPECT, and MRI often provides precise localization of seizure foci.
- The greatest challenge in performing ictal single-photon emission computed tomography for imaging in epilepsy is in injecting radiotracer as close to the time of seizure onset as possible.

Case 12-3

A 54-year-old woman with increasing frequency of seizures presented as a candidate for epilepsy surgery. Her symptomatology was stereotypic, with an aura of fear followed by loss of contact with her right hand, oral automatisms, and left hand dystonic posturing, all lasting 2 to 3 minutes. MRI revealed no temporal structural abnormality, but showed small occipital areas of cortical dysplasia. EEG revealed interictal sharp waves and intermittent rhythmic delta activity in the right temporal region. Fludeoxyglucose positron emission tomography (FDG-PET) in transverse (**Figure 12-4A**) and coronal planes (**Figure 12-4B**) revealed right temporal hypometabolism in both allocortex and neocortex. Ictal activation images (**Figures 12-4C** and **12-4D**) revealed focal ictal activation in the right anterior medial temporal lobe. Invasive electrophysiologic studies were deemed unnecessary given the correlative diagnostic information.

Comment. This case illustrates the key role neuromolecular imaging plays in the presurgical evaluation of patients with epilepsy. When all diagnostic information is congruent, expensive and invasive diagnostics, such as subdural electrode grids or depth electrodes, can often be avoided.

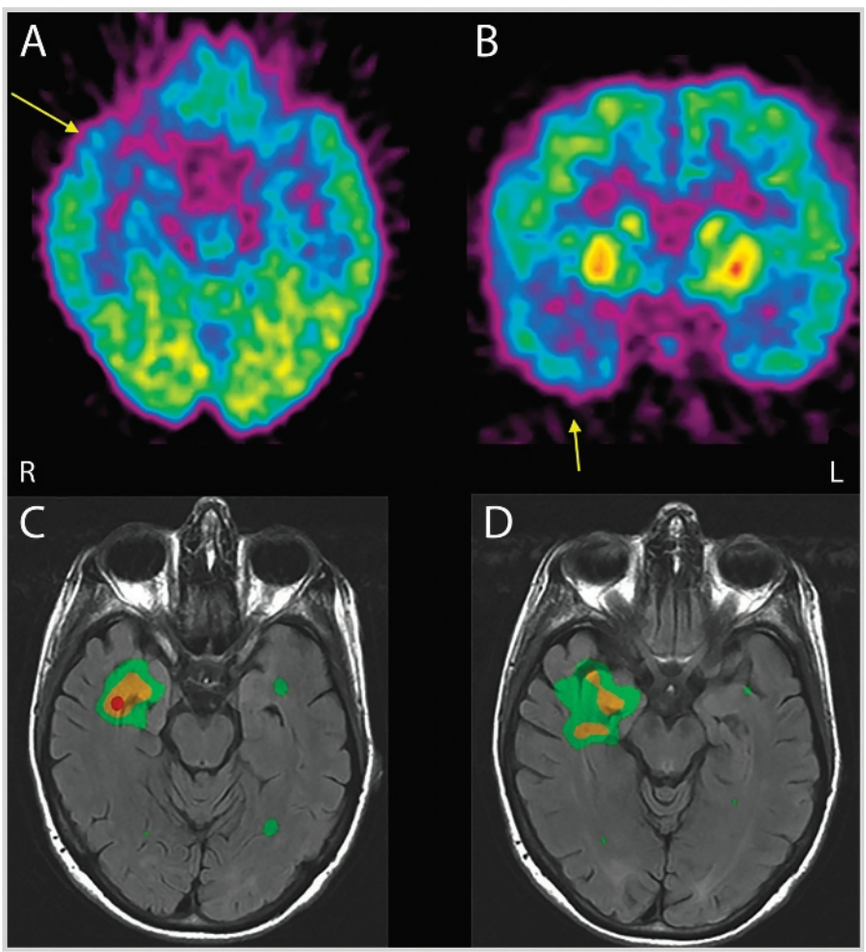

FIGURE 12-4 Neuromolecular imaging of the patient in Case 12-3 includes ictal fludeoxyglucose positron emission tomography (FDG-PET) (*A*, transverse; *B,* coronal), and ictal activation images (*C*, transverse; *D*, transverse, 5 mm dorsal to *C*). There is glucose hypometabolism in the right temporal lobe (*arrows, A, B*). The ictal activation images were generated from ictal and interictal bicisate single-photon emission computed tomography (SPECT) images. Both SPECT images are put into the same stereotactic space of the MRI, followed by proportional normalization, which then allows subtraction of the interictal image volume from the ictal image volume, leaving those regions that show increased perfusion due to ictus. The ictal activation images help to identify the location of seizure foci. The only coloration in *panel C* and *panel D* indicates the ictal activation. The processed SPECT is registered to a fluid-attenuated inversion recovery (FLAIR) sequence MRI, which is displayed in gray scale. In *panel A* and *panel B*, bright intensity or hot coloration (*red, yellow*) in PET indicates high tracer localization and higher amounts of glucose metabolism. Low intensity or cold coloration (*purple, blue*) indicates low amounts. In panel *C* and panel *D*, *red* and *orange* indicate high ictal activation. No color indicates no ictal activation.

corticobasal degeneration, and other types of frontotemporal dementia; and the secondary parkinsonian syndromes caused by drugs, vascular disease, or normal pressure hydrocephalus. Even tremor disorders, such as essential tremor, can enter the differential diagnosis.

The indications for neuromolecular imaging include the early diagnosis and differential diagnosis of parkinsonism. Currently, four radiotracers are clinically available in the United States with proven utility for these indications. These include exametazime and bicisate for cerebral perfusion SPECT, ioflupane for DAT imaging, and FDG for regional glucose metabolism. Each neuromolecular imaging type will show changes that reflect a hypodopaminergic state. The perfusion and metabolism tracers will also show regional dysfunction from disease involvement in other neuronal elements. The deficiency of dopamine, induced in earlier stages of the Lewy body diseases, will result in hyperperfusion or hypermetabolism within the striatum (**Figure 12-5**). This hyperfunction may also be seen from neuroleptic medication. All the other parkinsonism disorders typically cause hypofunction in the striatum. Only ioflupane I 123 provides a direct measure of the loss of dopamine innervation to the striatum.

The differential diagnostic utility of neuromolecular imaging results from the different patterns seen for different disorders. This is the principle used in the clinic for visual interpretation of these studies. It also underlies the published neuromolecular imaging literature. For validation, these patterns must be compared to some gold standard. Very few studies have used the best gold standard, which is postmortem tissue confirmation. In lieu of tissue diagnosis, most studies have used consensus clinical criteria

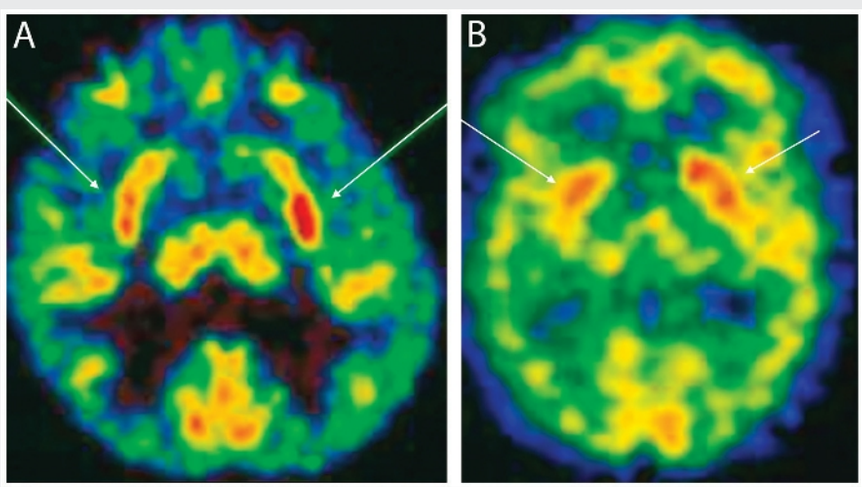

FIGURE 12-5 Two different 65-year-old men with stage 3 Parkinson disease, one scanned with fludeoxyglucose positron emission tomography (FDG-PET) (*A*) and the other with bicisate single-photon emission computed tomography (SPECT) (*B*). Both were withdrawn from dopaminergic therapy prior to neuromolecular imaging. Mild hypermetabolism (*A, arrows*) and hyperperfusion (*B, arrows*) can be seen in the striatum. This is often worse in the posterior inferior lenticular nuclei (*A*). This hyperfunction is absent in the neurodegenerative atypical parkinsonian syndromes, but it is seen in dementia with Lewy bodies. Bright intensity or hot coloration (*red, yellow*) indicates high tracer localization and thus higher amounts of glucose metabolism (*A*) and perfusion (*B*). Low intensity or cold coloration (*black, blue*) indicates low amounts.

KEY POINTS

- Differential diagnostic information for parkinsonism is provided by the pattern of striatal and cortical uptake of neuromolecular imaging tracers.
- The identification of loss of dopamine transporter and the pattern of that loss help to distinguish neurodegenerative parkinsonism from secondary parkinsonism caused by drugs and even from tremor disorders such as essential tremor.

developed by professional organizations, along with detailed patient follow-up for 0.5 to 3 years following the imaging. Such methodology has proven adequately valid upon direct examination.[28] There have also been two types of image analysis in the literature, visual examination of images by an expert versus applied computer methodology. The former replicates what occurs in the clinic, while the second is a field in development. Not surprisingly, the reported findings of the two methodologies are very similar because both begin with the same information: the images.

With clinical diagnosis consensus criteria as gold standard, FDG-PET is able to distinguish PD from atypical parkinsonian syndromes with greater than 90% accuracy, using expert visual analysis.[27,29,30] Visual analysis of FDG-PET can also discriminate between the atypical parkinsonian syndromes MSA, PSP, and corticobasal degeneration, with greater than 75% sensitivity and 90% specificity overall.[27,31] Concordance with clinical diagnosis was reported of 80% for MSA, 93.3% for PSP, and 100% for corticobasal degeneration in 136 parkinsonian patients.[29] Another study using similar methodology reported sensitivities/specificities of 77%/97% for MSA, 74%/95% for PSP, and 75%/92% for corticobasal degeneration in 95 parkinsonian patients.[30] The one recent study that used postmortem tissue diagnosis as the gold standard reported concordance of FDG-PET with tissue diagnosis in seven patients with PSP and one patient with corticobasal degeneration.[32] More study is needed on this, particularly with regard to concordance to postmortem gold standards, but the findings to date support the usefulness of FDG-PET in parkinsonism diagnosis. Little has been published on the role of perfusion SPECT in parkinsonism in the past 5 years, with this literature being mature but indicating a role for perfusion SPECT in these disorders.

Beyond visual interpretation, a number of studies have used computerized methods for analyzing FDG-PET images of parkinsonism. These methods have included voxel-based methods in which statistical analysis is applied to each volume element, or voxel, of the image, comparing the results to a database of normal subjects.[29] Other techniques have applied multivariate analyses to define neuronal networks based on how brain regions covary together.[33] Although there have been reported findings of a similar nature as that reported with visual analysis, it is the author's opinion that this computerized analysis field needs to mature further before there can be any consideration for its usefulness in the clinical arena.

Ioflupane I 123 has been shown by histopathology in animals and humans to bind to the DAT on presynaptic dopamine terminals. Loss of this binding is a surrogate marker of the loss of nigrostriatal terminals.[34,35] A high correlation ($R = 0.65$) exists between DAT imaging and the density of dopamine neurons in the substantia nigra. Parkinsonism can be a difficult differential diagnosis.[27] The identification of loss of DAT and the pattern of that loss help to distinguish neurodegenerative parkinsonism from secondary parkinsonism caused by drugs and even from tremor disorders such as essential tremor (**Figure 12-6**). DAT imaging using visual analysis has been reported to help distinguish vascular parkinsonism from PD with a 94% accuracy.[36] Each neurodegenerative process can have its own pattern, creating the potential to distinguish between them. Atypical parkinsonian syndromes and early DLB tend to have more homogenous and more symmetric involvement of the caudate and putamen than

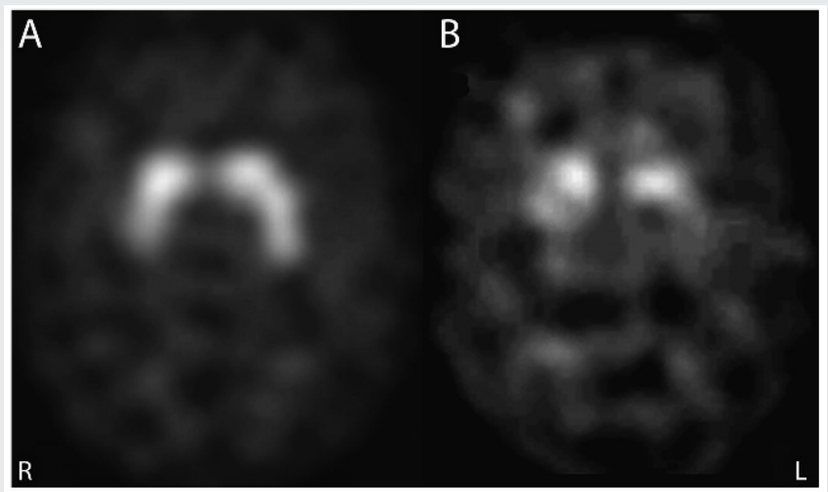

FIGURE 12-6 Ioflupane I 123 imaging of the dopamine transporter. *A*, Imaging of a 55-year-old man with a 5-year history of worsening hand tremor, worse on the right. There is normal ioflupane distribution through the cerebrum, making essential tremor the likely diagnosis. *B*, Imaging of a 39-year-old woman with a 1-year history of worsening tremors. Two findings are noted. Diminished contrast between the striatum and the rest of the brain due to decreased striatal uptake; these decreases are worse in the putamen, particularly posteriorly, than in the caudate. These findings are consistent with neurodegenerative parkinsonism. Although Parkinson disease is the most likely diagnosis, other atypical parkinsonian syndromes, such as multiple system atrophy, progressive supranuclear palsy, corticobasal degeneration, or frontotemporal dementia cannot be entirely ruled out. Bright intensity (*white*) indicates high tracer localization and thus higher dopamine transporter concentrations. Low intensity (*black*) indicates low amounts.

KEY POINTS

- Perfusion and metabolism imaging indirectly demonstrate the hypodopaminergic state by showing its synaptic consequences.
- Dopamine transporter imaging directly demonstrates the hypodopaminergic state by showing loss of dopaminergic nerve terminals.

PD. PD tends to have a posterior to anterior gradient of improving uptake within the striatum. However, a considerable overlap exists in the intrastriatal patterns, making distinction from other neurodegenerative parkinsonism difficult.[31] Given the phenotypic overlap of DLB and AD, DAT imaging has potential usefulness in this distinction. DAT imaging has 87% sensitivity and 94% specificity in distinguishing DLB from other dementias or controls.

CEREBROVASCULAR DISEASE

SPECT and PET are useful techniques for the evaluation of hemodynamic reserve in patients with severe cerebrovascular disease. SPECT allows assessment of cerebral perfusion. Using oxygen 15 (^{15}O) tracers, PET can measure cerebral blood flow, cerebral blood volume, and oxygen extraction fraction; the latter is a particularly good indicator of whether tissue is critically hypoperfused (the presence of increased oxygen extraction fraction means that the tissue is not receiving sufficient blood to its energy requirements). Three stages of hemodynamic compromise have been defined experimentally using ^{15}O PET tracers for measuring regional cerebral blood flow, blood volume, and oxygen extraction fraction.[37] Bicisate SPECT is capable of defining these three stages as well. Stage 0 is the absence of abnormality due to presence of collateral flow channels. In stage I, a tissue vasodilatation restores regional flow to normal but results in increased regional blood volume and decreased vascular reserve. Stage II has increased blood volume, decreased vascular reserve, and decreased blood flow or perfusion.

KEY POINT

- Cerebral perfusion single-photon emission computed tomography involves the simultaneous assessment of two physiologic processes, neuronal activity and the state of the vascular tree. Techniques to disentangle the cerebral perfusion single-photon emission computed tomography signal into neuronal function versus vascular disease induce a dilatation in responsive vascular beds by interventions that provoke tissue acidosis.

Cerebral perfusion SPECT involves the simultaneous assessment of two physiologic processes, neuronal activity and the state of the vascular tree. Techniques to disentangle the cerebral perfusion SPECT signal into neuronal function versus vascular disease induce a dilatation in responsive vascular beds by interventions that provoke tissue acidosis. Available options are the carbonic anhydrase inhibitor acetazolamide, which induces a metabolic acidosis, and inhalation of carbon dioxide–enriched gas, which induces a respiratory acidosis. The presence of compromised vascular reserve can be determined by comparing the perfusion before and after the vasodilatory challenge. Because vessels in ischemic territories will already be dilated, the vasodilatory challenge will result in lesser increase in perfusion in that area, indicating diminished vascular reserve (**Figure 12-7**). The increase in perfusion after the challenge is variable; in the author's experience, it is between 10% and 50%. This amount of activation is sufficient for diagnostic purposes.

The two main perfusion SPECT radiopharmaceuticals currently in use are exametazime Tc 99m and bicisate Tc 99m. Their cellular uptake mechanisms are different, which results in significantly different imaging capabilities. Only bicisate has a brain cell–specific uptake mechanism, based on one or more esterases only expressed within brain cells. The main uptake and retention mechanism for exametazime is glutathione chelation. Glutathione is present in all cells of the body, including inflammatory cells, meningeal cells, and fibrocytes. Most

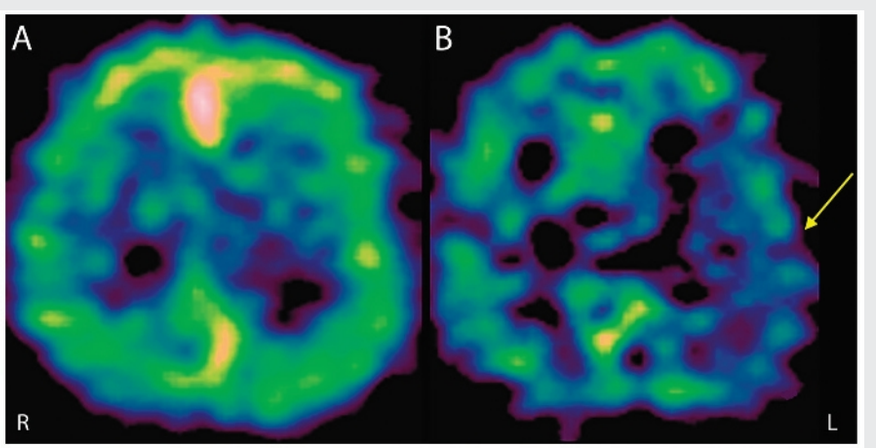

FIGURE 12-7 Imaging of a 49-year-old man who had undergone sacrifice of the left internal carotid artery for aneurysms that could not be treated endovascularly. Subsequently, the patient had two episodes of right arm shaking. The differential diagnosis was transient ischemic attacks versus seizure. The possible need for extracranial-intracranial bypass was discussed. Only heterogeneous multifocal white matter hypoperfusion is evident on the rest images of the bicisate vascular reserve cerebral activation perfusion single-photon emission computed tomography (SPECT) study (*A*), consistent with small vessel disease. However, after administration of the stress agent acetazolamide, a clear-cut middle cerebral artery territory hypoperfusion is evident (*B, arrow*), indicating vascular reserve compromise. It was likely the right arm shaking episodes were transient ischemic attacks. In the awake resting state, collateralization and middle cerebral artery tree vasodilatation are able to compensate for the hindered internal carotid artery flow. These compensations may not be adequate in states of decreased perfusion pressure (eg, sleep). Bright intensity or hot coloration (*white, yellow*) indicates high tracer localization and thus higher amounts of perfusion. Low intensity (*black, purple, blue*) indicates low amounts.

of the earlier literature in acute stroke that showed low diagnostic accuracies for perfusion SPECT used exametazime. Because of the difference of brain cell uptake mechanisms, brain cell viability, and, thus, reversible ischemia, is only reliably revealed by bicisate.

In acute stroke, two tissues are threatened: the ischemic core and the surrounding tissue, the penumbra. Although the fates are initially uncertain, much of the ischemic core will go on to infarction while the ischemic penumbra retains the potential for salvage. Stroke evolution over time is in major part related to propagation of infarction within these threatened tissues. SPECT with either exametazime or bicisate within the first 8 hours of acute stroke presentation has a positive predictive value of 90%, with reported sensitivities of 61% to 74% and specificities of 88% to 98%.[37] Twenty patients were evaluated with bicisate SPECT prior to IV recombinant tissue-type plasminogen activator (rtPA) therapy.[38] Brain regions with bicisate concentrations that were 15% to 53% that of the contralateral side went on to infarct despite rtPA therapy. Values of 45% to 83% indicated reversible ischemia salvageable from death following treatment. Values of 45% to 52% uptake were taken as the threshold for viability and therapy triage.[38] Exametazime-SPECT 1 hour following rtPA therapy in 35 patients was also predictive of outcome, with hypoperfusion associated with poor outcome.[39] Bicisate SPECT can also be used in the acute setting to distinguish a transient ischemic attack from an evolving stroke by using a cutoff uptake value of 70% or greater relative to the homologous region of the contralateral hemisphere.[40] In the subacute phase of stroke, bicisate retains its advantage over exametazime by its specificity of cell uptake mechanism. Exametazime may show higher apparent perfusion than bicisate because exametazime is taken up not just by brain cells but also by other cell types, such as inflammatory cells, fibrocytes, and other mesenchymal elements.

SPECT might also be useful in the evaluation of patients with suspected vascular cognitive impairment. Currently, the diagnosis of vascular dementia or vascular cognitive impairment is supported by MRI, which identifies tissue structural injury, such as gray or white matter infarcts or white matter hyperintensities. These methods are not sensitive to the presence of active ischemia before tissue injury, particularly that from small vessel disease. Measuring cerebral hemodynamic reserve may facilitate the etiologic diagnosis of cognitive impairment and help to address risk factor management. However, this application for SPECT remains mostly investigational.[41]

TRAUMATIC BRAIN INJURY

In the past few years, the public has been made aware of the role of repetitive TBI in causing long-term morbidity in athletes of contact sports. This clinical syndrome, called chronic traumatic encephalopathy, has most dramatically been demonstrated in former National Football League players.[42] However, TBI occurs throughout the population by various means, including motor vehicle accidents, assaults, and even falls in those with or without gait impairment. Following concussion or mild TBI, patients often are left with persistent symptoms that profoundly compromise their quality of life. CT and MRI often show no abnormalities.

These injuries occur due to differential brain acceleration and momentum relative to other tissues. Concussion results from rotational or angular acceleration of the brain. Contusion is

KEY POINT

■ The regions most often involved in traumatic brain injury include polar and orbital frontal lobes, polar and inferior temporal lobes, and dorsal frontal and parietal lobes. Less common areas include the perisylvian regions and inferior cerebellum.

a more forceful process, with actual macroscopic schism of tissue. The brain impacts surrounding structures, typically the inner table of the skull, but the meninges are also involved. Shear or strain forces also propagate within the brain itself, again due to a differential acceleration or momentum. White matter shear or strain injuries are one example. Most of these brain injuries are contrecoup injuries. Neuromolecular imaging shows decreased perfusion and metabolism at the sites of brain injury, typically in the polar and orbital frontal and temporal lobes, the dorsal vertex of the frontal and parietal lobes where glide contusions occur, and, less commonly, in the perisylvian regions and inferior cerebellum. However, injury can potentially occur anywhere in the cerebrum. Bicisate SPECT and FDG-PET have high sensitivity for detecting sites of injury because their imaging signal requires intracellular uptake of radiopharmaceuticals. Absence of cells or cellular dysfunction results in decreased radiopharmaceutical localization. Regional changes have been concordant with neuropsychological findings.[43] SPECT outperformed both CT and MRI and had high positive predictive value and near 100% negative predictive value for the continued presence of clinical symptoms at 3-month intervals after the injury.[44] In the author's experience, the location and pattern of physiologic changes on PET and SPECT in mild TBI include wedge defects and regional decreases incongruent with levels of perfusion or metabolism elsewhere in the cerebrum (**Figure 12-8**).

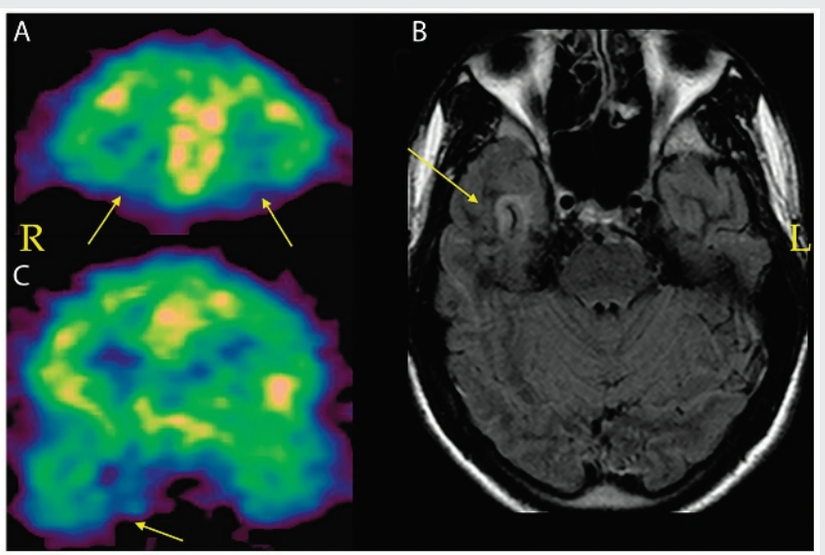

FIGURE 12-8 Imaging of a 22-year-old man with persistent cognitive and affective difficulties following a motor vehicle accident 1.5 years ago. His school performance had deteriorated, and he was anxious with a depressed mood, not typical for him prior to the accident. *A*, Bicisate single-photon emission computed tomography (SPECT) shows hypoperfusion in the orbital frontal cortices, where subtle parasagittal wedge defects are also seen (*arrows*). *B*, Fluid-attenuated inversion recovery (FLAIR) MRI shows a long T2 lesion in the right inferior temporal lobe (*arrow*) and no other findings. Bilateral inferior temporal cortex hypoperfusion can also be seen where a wedge defect is evident at the site of long T2 (*C, arrow*). In *panel A* and *panel C*, bright intensity or hot coloration (*white, yellow*) in SPECT indicates high tracer localization and thus higher amounts of perfusion. Low intensity or cold coloration (*purple, blue*) indicates low amounts.

CONCLUSION

Neuromolecular imaging is physiologic imaging of the cerebrum. Both basal physiologic and specific neurochemical systems can be examined. The literature has shown high diagnostic accuracy in a wide range of disorders, including dementia, brain tumors, epilepsy, parkinsonism, cerebrovascular disease, and TBI. Expanding utility in other disorders will likely be shown in the future. New radiopharmaceuticals tracing new and different physiologic processes are expected.

REFERENCES

1. Frisoni GB, Bocchetta M, Chételat G, et al. Imaging markers for Alzheimer disease: which vs how. Neurology 2013;81(5):487–500. doi:10.1212/WNL.0b013e31829d86e8.
2. Reiman EM, Jagust WJ. Brain imaging in the study of Alzheimer's disease. Neuroimage 2012;61(2):505–516. doi:10.1016/j.neuroimage.2011.11.075.
3. McKhann GM, Knopman DS, Chertkow H, et al. The diagnosis of dementia due to Alzheimer's disease: recommendations from the National Institute on Aging-Alzheimer's Association workgroups on diagnostic guidelines for Alzheimer's disease. Alzheimers Dement 2011;7(3):263–269. doi:10.1016/j.jalz.2011.03.005.
4. Albert MS, DeKosky ST, Dickson D, et al. The diagnosis of mild cognitive impairment due to Alzheimer's disease: recommendations from the National Institute on Aging-Alzheimer's Association workgroups on diagnostic guidelines for Alzheimer's disease. Alzheimers Dement 2011;7(3):270–279. doi:10.1016/j.jalz.2011.03.008.
5. Davison CM, O'Brien JT. A comparison of FDG-PET and blood flow SPECT in the diagnosis of neurodegenerative dementias: a systematic review. Int J Geriatr Psychiatry 2014;29(6):551–561. doi:10.1002/gps.4036.
6. de Souza LC, Lehéricy S, Dubois B, et al. Neuroimaging in dementias. Curr Opin Psychiatry 2012;25(6):473–479. doi:10.1097/YCO.0b013e328357b9ab.
7. Yeo JM, Lim X, Khan Z, Pal S. Systematic review of the diagnostic utility of SPECT imaging in dementia. Eur Arch Psychiatry Clin Neurosci 2013;263(7):539–552. doi:10.1007/s00406-013-0426-z.
8. Risacher SL, Saykin AJ. Neuroimaging biomarkers of neurodegenerative diseases and dementia. Semin Neurol 2013;33(4):386–416. doi:10.1055/s-0033-1359312.
9. Petersen RC, Aisen P, Boeve BF, et al. Mild cognitive impairment due to Alzheimer disease in the community. Ann Neurol 2013;74(2):199–208. doi:10.1002/ana.23931.
10. Roberts RO, Cha RH, Mielke MM, et al. Risk and protective factors for cognitive impairment in persons aged 85 years and older. Neurology 2015;84(18):1854–1861. doi:10.1212/WNL.0000000000001537.
11. White LR, Edland SD, Hemmy LS, et al. Neuropathologic comorbidity and cognitive impairment in the Nun and Honolulu-Asia Aging Studies. Neurology 2016;86(11):1000–1008. doi:10.1212/WNL.0000000000002480.
12. Arnaldi D, Morbelli S, Morrone E, et al. Cognitive impairment in degenerative parkinsonisms: role of radionuclide brain imaging. Q J Nucl Med Mol Imaging 2012;56(1):55–67.
13. Matsuda H, Imabayashi E. Molecular neuroimaging in Alzheimer's disease. Neuroimaging Clin N Am 2012;22(1):57–65, viii. doi:10.1016/j.nic.2011.11.005.
14. Bloudek LM, Spackman DE, Blankenburg M, Sullivan SD. Review and meta-analysis of biomarkers and diagnostic imaging in Alzheimer's disease. J Alzheimers Dis 2011;26(4):627–645. doi:10.3233/JAD-2011-110458.
15. Miletich RS. Positron emission tomography for neurologists. Neurol Clin 2009;27(1):61–88, viii. doi:10.1016/j.ncl.2008.09.004.
16. Horky LL, Treves ST. PET and SPECT in brain tumors and epilepsy. Neurosurg Clin N Am 2011;22(2):169–184, viii. doi:10.1016/j.nec.2010.12.003.
17. Alexiou GA, Tsiouris S, Voulgaris S, et al. Glioblastoma multiforme imaging: the role of nuclear medicine. Curr Radiopharm 2012;5(4):308–313.
18. Chierichetti F, Pizzolato G. 18F-FDG-PET/CT. Q J Nucl Med Mol Imaging 2012;56(2):138–150.
19. Ryken TC, Aygun N, Morris J, et al. The role of imaging in the management of progressive glioblastoma: a systematic review and evidence-based clinical practice guideline. J Neurooncol 2014;118(3):435–460. doi:10.1007/s11060-013-1330-0.
20. Chernov MF, Ono Y, Abe K, et al. Differentiation of tumor progression and radiation-induced effects after intracranial radiosurgery. Acta Neurochir Suppl 2013;116:193–210. doi:10.1007/978-3-7091-1376-9_29.
21. Crippa F, Alessi A, Serafini GL. PET with radiolabeled aminoacid. Q J Nucl Med Mol Imaging 2012;56(2):151–162.

KEY POINT

- Neuromolecular imaging has high sensitivity for the detection of traumatic brain injury and often shows injury when CT and MRI are negative.

22. Morales-Chacon LM, Alfredo Sanchez Catasus C, Minou Baez Martin M, et al. Multimodal imaging in nonlesional medically intractable focal epilepsy. Front Biosci (Elite Ed) 2015;7:42–57.

23. Kumar A, Chugani HT. The role of radionuclide imaging in epilepsy, part 1: sporadic temporal and extratemporal lobe epilepsy. J Nucl Med 2013;54(10):1775–1781. doi:10.2967/jnumed.112.114397.

24. Kumar A, Chugani HT. The role of radionuclide imaging in epilepsy, part 2: epilepsy syndromes. J Nucl Med 2013;54(11):1924–1930. doi:10.2967/jnumed.113.129593.

25. So EL, O'Brien TJ. Peri-ictal single-photon emission computed tomography: principles and applications in epilepsy evaluation. Handb Clin Neurol 2012;107:425–436. doi:10.1016/B978-0-444-52898-8.00027-6.

26. Rizzo G, Copetti M, Arcuti S, et al. Accuracy of clinical diagnosis of Parkinson disease. A systematic review and meta-analysis. Neurology 2016;86(6):566–576. doi:10.1212/WNL.0000000000002350.

27. Meyer PT, Hellwig S. Update on SPECT and PET in parkinsonism—part 1: imaging for differential diagnosis. Curr Opin Neurol 2014;27(4):390–397. doi:10.1097/WCO.0000000000000106.

28. Hughes AJ, Daniel SE, Ben-Shlomo Y, Lees AJ. The accuracy of diagnosis of parkinsonian syndromes in a specialist movement disorder service. Brain 2002;125(pt 4):861–870. doi:10.1093/brain/awf080.

29. Tripathi M, Dhawan V, Peng S, et al. Differential diagnosis of parkinsonian syndromes using F-18 fluorodeoxyglucose positron emission tomography. Neuroradiology 2013;55(4):483–492. doi: 10.1007/s00234-012-1132-7.

30. Hellwig S, Amtage F, Kreft A, et al. [^{18}F]FDG-PET is superior to [^{123}I]IBZM-SPECT for the differential diagnosis of parkinsonism. Neurology 2012;79(13):1314–1322. doi:10.1212/WNL.0b013e31826c1b0a.

31. Booij J, Teune LK, Verberne HJ. The role of molecular imaging in the differential diagnosis of parkinsonism. Q J Nucl Med Mol Imaging 2012;56(1):17–26.

32. Zalewski N, Botha H, Whitwell JL, et al. FDG-PET in pathologically confirmed spontaneous 4R-tauopathy variants. J Neurol 2014;261(4):710–716. doi:10.1007/s00415-014-7256-4.

33. Niethammer M, Feigin A, Eidelberg D. Functional neuroimaging in Parkinson's disease. Cold Spring Harb Perspect Med 2012;2(5):a009274. doi:10.1101/cshperspect.a009274.

34. Tatsch K, Poepperl G. Nigrostriatal dopamine terminal imaging with dopamine transporter SPECT: an update. J Nucl Med 2013;54(8):1331–1338. doi:10.2967/jnumed.112.105379.

35. Walker Z, Cummings JL. [123I]N-ω-fluoropropyl-2β-carbomethoxy-3β-(4-iodophenyl)nortropane single-photon emission computed tomography brain imaging in the diagnosis of dementia with Lewy bodies. Alzheimers Dement 2012;8(1):74–83. doi:10.1016/j.jalz.2011.08.003.

36. Benitez-Rivero S, Marin-Oyaga VA, Garcia-Solis D, et al. Clinical features and 123I-FP-CIT SPECT imaging in vascular parkinsonism and Parkinson's disease. J Neurol Neurosurg Psychiatry 2013;84(2):122–129. doi:10.1136/jnnp-2012-302618.

37. Heiss WD. Radionuclide imaging in ischemic stroke. J Nucl Med 2014;55(11):1831–1841. doi:10.2967/jnumed.114.145003.

38. Nakano S, Iseda T, Ikeda T, et al. Thresholds of ischemia salvageable with intravenous tissue plasminogen activator therapy: evaluation with cerebral blood flow single-photon emission computed tomographic measurements. Neurosurgery 2000;47(1):68–73.

39. Abumiya T, Katoh M, Moriwaki T, et al. Utility of early post-treatment single-photon emission computed tomography imaging to predict outcome in stroke patients treated with intravenous tissue plasminogen activator. J Stroke Cerbrovasc Dis 2014;23(5):896–901. doi:10.1016/j.jstrokecerebrovasdis.2013.07.028.

40. Berrouschot J, Barthel H, Hesse S, et al. Differentiation between transient ischemic attack and ischemic stroke within the first six hours after onset of symptoms by using ^{99m}Tc-ECD-SPECT. J Cereb Blood Flow Metab 1998;18(8):921–929. doi:10.1097/00004647-199808000-00013.

41. Farid K, Petras S, Ducasse V, et al. Brain perfusion SPECT imaging and acetazolamide challenge in vascular cognitive impairment. Nucl Med Commun 2012;33(6):571–580. doi:10.1097/MNM.0b013e328351d583.

42. Mez J, Stern RA, McKee AC. Chronic traumatic encephalopathy: where are we and where are we going? Curr Neurol Neurosci Rep 2013;13(12):407. doi:10.1007/s11910-013-0407-7.

43. Lin AP, Liao HJ, Merugumala SK, et al. Metabolic imaging of mild traumatic brain injury. Brain Imaging Behav 2012;6(2):208–223. doi:10.1007/s11682-012-9181-4.

44. Raji CA, Tarzwell R, Pavel D, et al. Clinical utility of SPECT neuroimaging in the diagnosis and treatment of traumatic brain injury: a systematic review. PLoS One 2014;9(3):e91088. doi:10.1371/journal.pone.0091088.